All-in-one dispersion-compensating saturable absorber mirror for compact femtosecond laser sources

D. Kopf, G. Zhang, R. Fluck, M. Moser, and U. Keller

Ultrafast Laser Physics Laboratory, Institute of Quantum Electronics, Swiss Federal Insititute of Technology, ETH Hönggerberg–HPT, CH-8093 Zürich, Switzerland

Received September 15, 1995

A molecular-beam-epitaxy-grown semiconductor saturable absorber mirror with integrated dispersion compensation, based on a Gires–Tournois structure, is demonstrated. This dispersion-compensating saturable absorber mirror generated 160-fs pulses with 25-mW average power from a simple diode-pumped Cr:$LiSrAlF_6$ laser without any additional dispersion compensation. © 1996 Optical Society of America

Compactness and cost effectiveness are important for real-world femtosecond laser systems. Diode pumping is one key step in this direction, and as a next step we use semiconductor saturable absorbers to passively start and stabilize soliton mode locking.[1] In the case of soliton mode locking the dominant pulse-forming mechanism is soliton formation, and the saturable absorber simply starts and stabilizes this process. In contrast to Kerr-lens mode locking,[2] this technique works over the full cavity stability regime, and no critical cavity adjustments are necessary. Femtosecond pulse generation requires dispersion compensation, for which intracavity prisms are most commonly used, adding more complexity to the system. In this Letter we demonstrate a novel dispersion-compensating saturable absorber mirror (D-SAM) that combines both saturable absorption and negative group-velocity dispersion (GVD) in one element.[3] The D-SAM generates femtosecond pulses by the simple replacement of one end mirror of a cw oscillator, without the need for any further dispersion compensation such as a prism pair. We give design criteria for the D-SAM, which is based on a Gires–Tournois structure[4] and can be extended to other dispersion-compensation techniques such as chirped mirrors.[5]

As demonstrated earlier, semiconductors offer many possibilities for custom-designed key parameters of a saturable absorber, such as impulse response with two or more time constants, saturation fluence, and insertion loss.[6–8] However, previous designs have relied only on pure absorption of the semiconductor.[6,8,9] The D-SAM design extends the design criteria to dispersion compensation as well. The D-SAM (inset in Fig. 1) consists of a metal-oxide chemical-vapor-deposition-grown Bragg mirror ($R > 99.5\%$) with a low-temperature (400 °C) molecular-beam-epitaxy-grown (MBE) 30-nm-thick saturable absorber layer ($Al_{0.06}Ga_{0.94}As$), sandwiched between two spacer layers (AlAs and $Al_{0.65}Ga_{0.35}As$) with a band-gap energy sufficiently high to be transparent for the laser wavelength. The saturable absorber shows a bitemporal impulse response with the two carrier relaxation times of 250 fs and 2.3 ps, respectively, as measured in a standard pump–probe setup.[6,7] The thickness of the saturable absorber layer is limited by the unbleached insertion loss of the material.[8] The total thickness of the spacer layers is chosen such that a Gires–Tournois-like Fabry–Perot cavity[4] is formed by the top semiconductor–air interface and the Bragg mirror as the two dominant reflecting surfaces. This Fabry–Perot structure has a resonance that is close to the laser wavelength $\lambda = 840$ nm. The resultant group delay around this resonance [solid curve in Fig. 2(a)] indicates that negative GVD of approximately $\partial T_g/\partial\omega = 400\ \mathrm{fs}^2$ is obtained at the laser wavelength. This is also confirmed by the measured group delay[10] (dashed curve), which is in good agreement with the design data.

The position of the saturable absorber layer inside the structure is an important design parameter. We would prefer to place the saturable absorber layer at a high field location (see the intensity plot in Fig. 3), such that the effective saturation fluence of the device is reduced. However, this would cause a pronounced absorption dip at the resonance wavelength [Fig. 2(b)], and the extra loss would push the lasing wavelength away from the negative GVD regime toward one of the two reflection maxima. Therefore we put the absorber layer close to the field minimum (Fig. 3). Different wavelengths have different field node positions, resulting from the Bragg-mirror-dependent phases (node positions indicated by arrows in Fig. 3). As we approach the resonance wavelength,

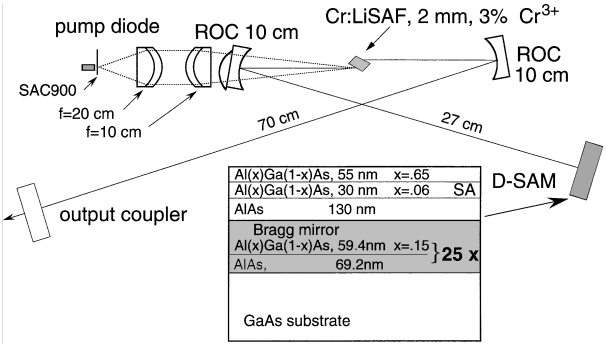

Fig. 1. Setup of femtosecond Cr:LiSAF laser with the D-SAM and the output coupler (1%) as end mirrors. Inset: structure of the D-SAM device. All layers except the saturable absorber (SA) layer are transparent at the laser wavelength. ROC, radius of curvature; SAC900, single-axis collimator microlens (Blue Sky Research).

0146-9592/96/070486-03$6.00/0

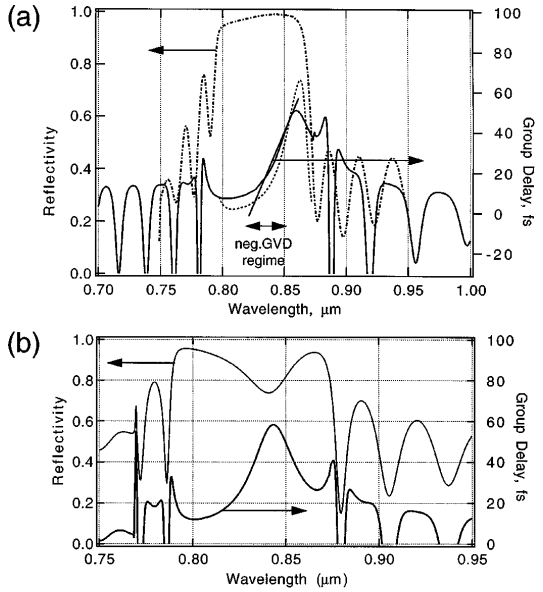

Fig. 2. (a) Measured reflectivity and group delay of the D-SAM (dashed curves) and the calculated group delay of the D-SAM (solid curve), where positive slope corresponds to negative GVD. (b) Calculated reflectivity curve and group delay for a design with the absorber layer (GaAs) positioned at the field maximum of the standing wave inside the Gires–Tournois structure, resulting in a strong absorption dip at the resonance. Laser operation will not be possible in the negative GVD regime because the Cr:LiSAF broad emission band will prefer lasing at one of the two reflection maxima.

the intensity maximum inside the D-SAM rises (see second set of arrows in Fig. 3), but at the same time the field node moves closer to the center of the absorbing layer, which reduces the absorption caused by the absorber layer. The resulting reflectivity curve as a function of wavelength no longer shows a dip [Fig. 2(a)], and the laser operates in the negative GVD regime. Similar to the case of the low-finesse antiresonant Fabry–Perot saturable absorber,[8,9,11] no further processing is required after the MBE, unlike with earlier saturable absorber designs such as the high-finesse antiresonant Fabry–Perot saturable absorber[6] and the thin antireflection-coated saturable absorber reflector.[12]

We chose Cr-doped $LiSrAlF_6$ (Cr:LiSAF) as the gain medium because of its low GVD, which is ~4 times lower than that of Ti:sapphire and other laser materials at $\lambda = 840$ nm. In addition, Cr:LiSAF has an emission bandwidth broad enough to support pulses in the tens-of-femtoseconds regime.[13–16] Therefore the pulse width in our experiment will be limited only by the characteristics of the D-SAM and not by the gain bandwidth.

The cavity is a standard Δ cavity (Fig. 1). The lasing mode size on the D-SAM has a 100-μm radius, according to *ABCD* matrix calculations. The pump arrangement is similar to that described in Ref. 15. The laser is compact and easy to align, as no intracavity prisms have to be used. Because the saturable absorber starts and stabilizes soliton mode locking,[1] the cavity is operated approximately in the middle of the cavity stability regime, unlike Kerr-lens mode locking, which tends to require critical cavity alignment for an optimized Kerr-lens effect.

We obtained transform-limited 160-fs pulses (Fig. 4) and, as a result of the low-insertion loss of the D-SAM ($< 1\%$), an average output power of 25 mW with an absorbed pump power of 300 mW from only one diode-laser pump source. The pulses were transform limited with a time–bandwidth product of 0.32, as we expect from soliton mode locking.[1] When we used two pump laser diodes, the average output power was 80 mW at an absorbed pump power of 650 mW. However, mode locking was no longer stable in this cavity arrangement, which we attribute to the increased pulse energy. A stable soliton requires shorter pulses for fixed GVD but increased pulse energy and self-phase modulation. However, at some point the D-SAM can no longer support negative GVD for the broader spectrum. In our experiment, we found that 160 fs was the minimum achievable pulse width. When we shortened the cavity's longer arm to 25 cm, the pulse energy dropped and the lasing mode size inside the gain medium increased, resulting in a reduced nonlinearity in the gain medium. In this higher-repetition-rate cavity we obtained stable 250-fs pulses at 80-mW average output power, consistent with the soliton mode-locking model.

The mode locking was observed to be stable over several hours. However, a decrease in output power and an occasional dropout occurred on this time scale. The D-SAM design ends with AlGaAs to air, which is subject to oxidation, and we attribute this damage effect to oxidation at the surface. As the intensity

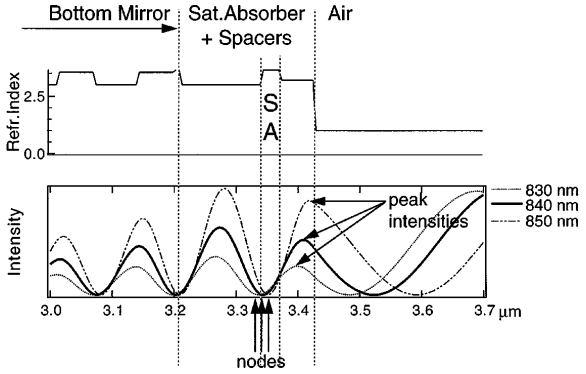

Fig. 3. Standing-wave pattern of intensity inside the D-SAM structure for three different wavelengths (lower graph) and corresponding refractive-index profile (upper graph). The three arrows indicate different intensity node and maxima locations for the three wavelengths. See Fig. 1 for details.

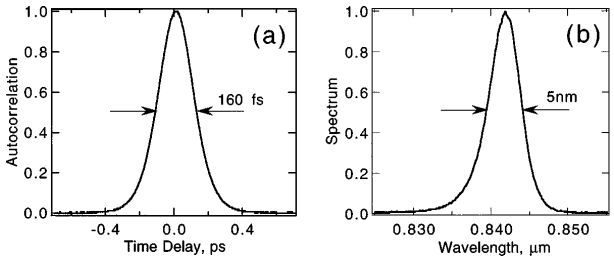

Fig. 4. Transform-limited mode-locking results: (a) noncollinear autocorrelation, (b) pulse spectrum. Solid curves, measured; dotted curves, sech^2 fit.

maximum is close to the surface, the design is particularly sensitive to any loss at the AlGaAs–air interface. We confirmed this by flowing dry nitrogen gas across the sample, which reduced the decrease in output power per hour by a factor of ≈4. Equivalently, a dielectric protection layer (10 nm of SiO evaporated on top of the D-SAM) reduced the degradation by approximately the same amount without changing the device's characteristics. However, for full protection the coating should be thicker than 10 nm, and additional surface treatment and passivation would be needed, which would change the reflectivity and group-delay curve. The reliability of AlGaAs surfaces has been investigated thoroughly in diode-laser research,[17] and dielectric protection coatings have been found to be a possible solution. Devices based on GaInAsP/GaAs material have also shown much better reliability than AlGaAs devices, since GaInAsP/GaAs has a smaller oxidation rate and small surface recombination velocity, which we regard as a possible solution in our case. A second reason for damage can be attributed to the high intensity at the interface (Fig. 3), which is fundamental to the Gires–Tournois structure. Surfaces in general have a lower damage threshold than bulk material[18]; therefore field-induced damage is most likely to occur at the interface in our case. This issue is still under investigation. However, damage has not been observed with low-finesse antiresonant Fabry–Perot saturable absorber designs[8,11] because of the field node at the surface, which increases the device's effective surface damage threshold.

We think that the D-SAM concept will be particularly interesting in the 1-μm wavelength region with narrow-bandwidth laser materials. Not only will oxidation be avoided with InGaAs/GaAs-based structure but the lasing wavelength will be determined within a few nanometers by the emission spectrum of a gain medium such as Nd:glass or Yb:YAG, both of which have been mode locked in the femtosecond regime with semiconductor saturable absorbers.[11,19] The use of narrower-bandwidth gain media does not require the D-SAM to be designed simultaneously for both minimum loss and negative GVD at the desired wavelength. It is sufficient to design the D-SAM for negative GVD over the emission spectrum of the gain medium, i.e., over 10–20 nm for Nd:glass. Therefore, unlike our design, the saturable absorber layer will not necessarily have to be put close to a field node, which no longer increases the effective saturation fluence. This will make the design easier and will help to overcome surface damage because the laser intensity incident upon the D-SAM can be reduced while the saturable absorber layer is still saturated.

In conclusion, we have demonstrated a MBE dispersion-compensating saturable absorber mirror generating 160-fs pulses from a diode-pumped Cr:LiSAF laser, without the use of any other dispersion compensation such as prisms. We have given design criteria for the D-SAM device, which combines both negative GVD and saturable absorption in one element, based on a Gires–Tournois-like structure with an integrated saturable absorber layer. The design was chosen for maximum reflectivity at a wavelength where negative GVD is provided at the same time, forcing the Cr:LiSAF laser to run in the negative GVD regime. We anticipate that narrower gain media such as Nd:glass, in contrast to Cr:LiSAF, would make the design of the D-SAM simpler because the gain medium defines the lasing wavelength rather than the D-SAM's reflectivity curve.

The authors thank Robert Szipöcs for the dispersion measurement and fruitful discussions, Christian Zemlin for help with some of the experimental setups, and Luigi Brovelli for the multilayer reflection calculation program. This research was supported by Swiss National Science Fund 21-39362.93.

M. Moser is also with the Paul Scherrer Institute, CH-8048 Zurich, Switzerland.

References

1. F. X. Kärtner and U. Keller, Opt. Lett. **20,** 16 (1995).
2. D. E. Spence, P. N. Kean, and W. Sibbett, Opt. Lett. **16,** 42 (1991).
3. D. Kopf, G. Zhang, M. Moser, and U. Keller, in *Conference on Lasers and Electro-Optics,* Vol. 15 of 1995 OSA Technical Digest Series (Optical Society of America, Washington, D.C., 1995), paper CPD41.
4. F. Gires and P. Tournois, C. R. Acad. Sci. Paris **258,** 6112 (1964).
5. R. Szipöcs, K. Ferencz, C. Spielmann, and F. Krausz, Opt. Lett. **19,** 201 (1994).
6. U. Keller, Appl. Phys. B **58,** 347 (1994).
7. L. R. Brovelli, U. Keller, and T. H. Chiu, J. Opt. Soc. Am. B **12,** 311 (1995).
8. I. D. Jung, L. R. Brovelli, M. Kamp, U. Keller, and M. Moser, Opt. Lett. **20,** 1559 (1995).
9. S. Tsuda, W. H. Knox, E. A. de Souza, W. Y. Jan, and J. E. Cunningham, Opt. Lett. **20,** 1406 (1995).
10. A. P. Kovacs, K. Osvay, Z. Bor, and R. Szipocs, Opt. Lett. **20,** 788 (1995).
11. C. Hönninger, G. Zhang, U. Keller, and A. Giesen, Opt. Lett. **20,** 2402 (1995).
12. L. R. Brovelli, I. D. Jung, D. Kopf, M. Kamp, M. Moser, F. X. Kärtner, and U. Keller, Electron. Lett. **31,** 287 (1995).
13. D. Kopf, K. J. Weingarten, L. Brovelli, M. Kamp, and U. Keller, Opt. Lett. **19,** 2143 (1994).
14. M. J. P. Dymott and A. I. Ferguson, Opt. Lett. **19,** 1157 (1994).
15. D. Kopf, K. J. Weingarten, L. R. Brovelli, M. Kamp, and U. Keller, in *Conference on Lasers and Electro-Optics,* Vol. 15 of 1995 OSA Technical Digest Series (Optical Society of America, Washington, D.C., 1995), paper CWM2.
16. M. J. P. Dymott and A. I. Ferguson, in *Conference on Lasers and Electro-Optics,* Vol. 15 of 1995 OSA Technical Digest Series (Optical Society of America, Washington, D.C., 1995), paper CWM1.
17. M. Fukuda, *Reliability and Degradation of Semiconductor Lasers and LEDs* (Artech, Boston, Mass., 1991).
18. W. Koechner, *Solid-State Laser Engineering* (Springer-Verlag, Berlin, 1988).
19. D. Kopf, F. X. Kärtner, K. J. Weingarten, and U. Keller, Opt. Lett. **20,** 1169 (1995).